

Chemistry and clumpiness in planetary nebulae

M.P. Redman¹, S. Viti², P. Cau^{3,4} and D.A. Williams¹

¹ Department of Physics & Astronomy, University College London, Gower Street, London WC1E 6BT, UK

² Istituto di Fisica dello Spazio Interplanetario, CNR, Via del Fosso Caveliere 100, 00133 Roma, Italy

³ Observatoire de Paris-Meudon, 92195 Meudon, France

⁴ Department of Meteorology, University of Reading, Earley Gate, P.O. Box 243, Reading RG6 6BB, UK

29 October 2018

ABSTRACT

We study the chemistry in the slow wind during the transition from AGB star to pre-planetary nebula (PPN) and planetary nebula (PN). We show that there is a very rich chemistry of degradation products created by photoprocessing, driven by the gradually hardening radiation field of the central star. Most of these products are, however, photodissociated during the PPN phase if the wind is smooth. By contrast, if the wind is clumpy, possibly because of clumpiness in the AGB atmosphere, then many of these degradation products survive into the PN phase. Thus, chemistry may be used to infer the existence of clumpiness in the AGB phase. We identify potential molecular tracers, and we note that, in the case of clumpiness, large molecules may survive the transport from the stellar atmosphere to the interstellar medium. We compare between our model results with observations of three objects at differing evolutionary stages: CRL618, NGC 7027 and the Helix nebula (NGC 7293).

Key words: ISM: globules - ISM: molecules - planetary nebulae: general - planetary nebulae: individual (Helix nebula, NGC 7027, CRL618)

1 INTRODUCTION

Nearby planetary nebulae are clearly observed to be clumpy (O'Dell et al. 2002) with perhaps the best known example being the Helix nebula (Meaburn et al. 1998; O'Dell & Handron 1996). The latter authors estimate that around half of the mass of the Helix nebula is contained in clumps. The origin of the clumps remains very unclear and there have been several models proposed for their generation. Dyson et al. (1989) suggested that the SiO maser spots observed in the atmospheres of AGB stars could be the first manifestation of clumps later observed in the planetary nebula. Other models involve clumps forming much later during the planetary nebula phases. Williams (1999) has shown how density fluctuations at an ionization front boundary can produce knots and tails when the ionization front switches locally from R-type to D-type (see e.g. Shu 1991 for a detailed discussion of ionization front types). Instabilities in the shell of ionized gas, with the instability being either Rayleigh-Taylor (Capriotti 1973) or 'thin layer' (García-Segura & Franco 1996), have also been proposed as mechanisms to form clumps.

Very recently, Huggins & Mauron (2002) have observed the envelopes of NGC 7027, the proto-typical young planetary nebula, and IRC+10216, the standard C-rich AGB star, in order to look for knots generated at the AGB phase. Since none were observed in these two objects, any envelope knots

must be very small or else they would be seen in scattered light. However, in the innermost regions of NGC 7027, the ionized and neutral material surrounding the ionized cavity are observed to be very clumpy and Huggins & Mauron (2002) suggest that the knots are formed as the complex (and poorly understood) transition from AGB wind to planetary nebula occurs. The models and explanations for the origin of the clumps can thus be separated into two types: those in which the clumps form early, before the PN is fully developed (Dyson et al. 1989; Huggins & Mauron 2002) and those in which the clumps form later during the PN stage (Williams 1999; García-Segura & Franco 1996; Capriotti 1973).

The chemical history of the clumps will depend on where and when they formed since the chemistry is sensitive to the radiation field, temperature and extinction of the clump gas. Molecular observations may thus offer the best way to establish the evolutionary history of the clumps and thus to differentiate between the two types of model. There has been rapid progress in recent years in characterising the chemistry of the post-AGB phases with many molecules being identified in young objects such as NGC 7027 (e.g. Hasegawa & Kwok 2001 and references therein) and several species observed in evolved PNe such as the Helix where, for example, Young et al. (1997) observed neutral carbon in the globules. Bachiller et al. (1997) observed molecules in clumps in a range of planetary nebulae at dif-

ferent evolutionary stages, allowing trends in the molecular abundances with age to be identified.

In this paper, we trace the chemical evolution of model clumps, assuming them to have formed early on in the history of the PN and compare the results from those expected if the clumps formed *in situ*. The aim is to identify observable species that can be used as discriminants between the two scenarios.

Our model is described in Section 2, and our results are presented, discussed and compared with observations in Section 3. We conclude in Section 4 that molecular tracers do exist in PPNe and PNe, and that some large molecules originating in the stellar atmosphere may survive the transition into the interstellar medium.

2 PHYSICAL AND CHEMICAL MODEL

The difference between a clumpy and non-clumpy model is that clump interiors will have a higher extinction than their surroundings. In the harsh environment of a planetary nebula this can help to shield molecules so that they survive for longer than if they were in the interclump gas. The chemical difference between clumps that are formed out of the planetary nebula gas and those that formed earlier is that in the latter case, complex molecules may be shielded and preserved long enough to be detectable in clumps. In the former case, all such molecules will have been destroyed as the extinction of the gas dropped as the PN evolved.

Howe et al. (1992) investigated the gas-phase chemistry in a carbon-rich AGB wind during its transition to a planetary nebula. This work was followed by a paper (Howe et al. 1994) investigating the formation of molecules in a dense, neutral globule such as those observed in the Helix nebula. Howe et al. (1994) ran equilibrium chemistry models for clumps with extinctions between 0 and 2.0, comparable to those of the Helix knots (Meaburn et al. 1998). They found that molecular abundances in the globule are enhanced with C₂H and CN at abundances that are possibly detectable in carbon-rich globules.

Here, we extend the work of Howe et al. (1994) in that the time-dependent chemistry is calculated, beginning with the rich chemistry of a carbon-rich AGB atmosphere. The molecular species are assumed to be locked into a clump with a density contrast with the surrounding medium. The chemistry of the clump is then traced as both it and the surrounding medium expand away from the star. At the final stage of the calculation, the clump and medium have similar properties to those of the Helix. As the knots in the Helix have a low extinction, the chemistry by this stage is tending towards that expected of a diffuse cloud with this initial composition. However, at intermediate stages, the rich initial chemistry should give rise to marked differences compared with that expected from a standard ISM mixture. Some of these molecules should be present in detectable quantities and if found, would argue for an early clump formation model. We follow the physical and chemical evolution of a parcel of gas (either clump or interclump material) as it moves out from the AGB atmosphere to the protoplanetary (PPN) and planetary nebula (PN) phases, ultimately merging with the interstellar medium.

In the AGB atmosphere, the number density and tem-

perature are on the order of 10¹² cm⁻³ and 10³ K, respectively. We assume that the clump/interclump density ratio is about 10 (Mauron & Huggins 2000 find the multiple shells in the envelope of IRC+10216 to have density contrasts of $\lesssim 10$), and that the size of the clump is comparable to a stellar radius (about 10¹³ cm). Thus, if the gas:dust ratio is similar to that in the interstellar medium, the visual extinction associated with a clump in the atmosphere is very large. The chemistry in the atmosphere is determined under thermodynamical equilibrium, and the relative abundances are fixed as the envelope expands and the density falls. At lower densities, however, thermodynamic equilibrium no longer applies and chemistry is driven by two-body reactions of ion-molecule and other types, as in conventional interstellar chemistry.

Since no chemical evolution occurs in the initial expansion, we begin our computation of the evolution at a later stage (time $t = t_1 = 100$ yr) at which the densities are low enough to be dominated by two-body reactions initiated by cosmic ray ionisation and by photoprocesses driven by the radiation field of the central star and by the ambient interstellar medium.

For simplicity, we use a power-law description of the physical development. We do not attempt to model the initiation and evolution of a clump. In a steady outflow at constant velocity, the density should fall off as t^{-2} . However, the density fall off in a clump may be slower. A $t^{-3/2}$ dependence gives a reasonable fit to typical densities through the PPN and PN stages (as observed by, e.g. Martin-Pintado et al. 1995; Meaburn et al. 1998). Therefore we adopt

$$n(t) = 10^7 \left(\frac{t}{t_1} \right)^{-3/2} \text{ cm}^{-3}, \quad (1)$$

for times $t > t_1$, where $t_1 = 100$ yr. On the assumption of constant clump mass throughout the expansion, this gives

$$r(t) = 10^{14} \left(\frac{t}{t_1} \right)^{1/2} \text{ cm}. \quad (2)$$

The visual extinction associated with a clump must therefore vary as t^{-1} , and we write

$$A_V = 10^2 \left(\frac{t}{t_1} \right)^{-1}. \quad (3)$$

The distance of the clump from the star is d , which in a steady flow must increase linearly with time:

$$d(t) = 10^{16} \left(\frac{t}{t_1} \right) \text{ cm}. \quad (4)$$

We adopt the following dependence of temperature on time, as it gives values for the PN clump temperatures comparable to the typical measured values (Martin-Pintado et al. 1995; Meaburn et al. 1998):

$$T(t) = 316 \left(\frac{t}{t_1} \right)^{-1/4} \text{ K}. \quad (5)$$

The radiation field experienced by the parcel of gas is initially dominated by the contribution from the central star, and later by that of the interstellar radiation field. We adopt the following expression, similar to that used by Howe et al. (1994), for the radiation field intensity χ ,

$$\chi = 0; D < 10^{16} \text{ cm}, \quad (6)$$

$$= 100\chi_{\text{ism}} \left(\frac{t}{t_1} \right)^{-2} + \chi_{\text{ism}}; D < 10^{16} \text{ cm}, \quad (7)$$

where we assume that χ_{ism} gives photorates as in the UMIST rate file (Millar et al. 1997, and discussed further below). There is some uncertainty in this, since the radiation field may be harder than that of the interstellar medium. We use the canonical cosmic ray ionisation rate of $\chi_{\text{ism}} = 1.3 \times 10^{-17} \text{ s}^{-1}$.

The evolution of the interclump medium can be followed in a very similar way to that of a clump. In this single-point calculation, the initial composition in the AGB atmosphere is the same as for a clump but the parcel of gas is assumed to have an initial density lower by a factor of 10 compared with the clump. The density falls off with the square of the distance from the star, as appropriate for a steady spherically symmetric flow.

$$n(t) = 10^6 \left(\frac{t}{t_1} \right)^{-2} \text{ cm}^{-3}. \quad (8)$$

A parcel of gas will then experience an extinction that varies as

$$A_V = 10^2 \left(\frac{t}{t_1} \right)^{-4/3}. \quad (9)$$

Since the clump and interclump medium will initially have the same temperature, it is assumed for simplicity that the interclump medium temperature is the same as that of the clump, and therefore varies as given by Equation 5. This is unlikely to be true in the later stages of the PN evolution when the interclump medium will be hotter than the clumps but this will only accelerate the destruction of those molecules that survived the drop in extinction. In the period of interest, the range of temperatures involved does not influence the chemistry very strongly.

The chemical model used is similar to the one employed in Viti & Williams (1999). However, we have made considerable changes to the chemistry. To all the basic species (O, C, CO etc.) we have added all the species (mainly hydrocarbons) that are thought to be abundant at the initial stage of the PPN; this chemistry also includes species that have an unpaired electron located on an internal or terminal carbon atom. For most of these additions, the UMIST rate file for gas phase reactions, involving several hundred species (Millar et al. 1997), and which is normally used routinely in our models, did not have a sufficient network of reactions. Therefore the formation and destruction routes were taken from Frenklach & Feigelson (1989). The reaction rates were fitted by using different formulae from the UMIST ones. To account for that, we have modified our code to include new rate coefficients calculations taken from Cau (2001). For some of those reactions, no rate coefficients are available and Frenklach & Feigelson (1989) determine them from the rate coefficients of their inverse reactions: we have employed the same method here. We have not included three-body reactions. We have also excluded reactions which use an ‘unspecified’ species as a collisional body causing de-excitation or dissociation. These may be of some relevance and should be included in further studies. Note that Frenklach & Feigelson (1989) also extrapolated their rate coefficients to temperatures very different from those at which they were measured.

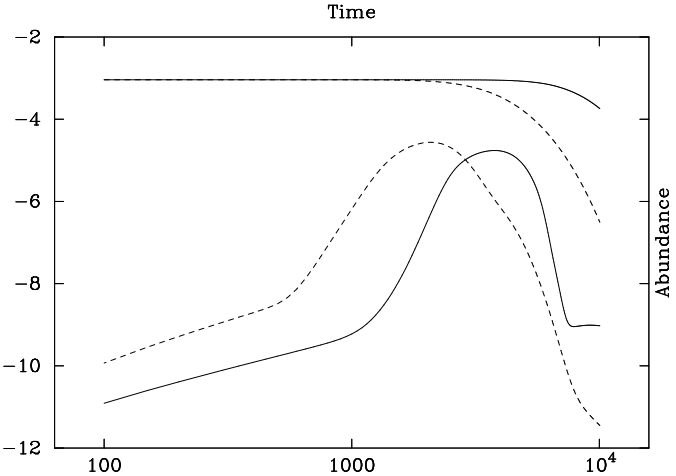


Figure 1. Clump (solid lines) and interclump (dashed lines) abundances for CO (uppermost solid line) and CN. The time is measured in years from the end of the AGB phase. The fractional abundance is with respect to the total number of hydrogen atoms. The object becomes a PPN after a few hundred years and by about 1000 years the object is a PN

3 RESULTS AND DISCUSSION

3.1 Predictions

We present in Figures 1-4 results of the calculations of the evolution of molecular fractional abundances in clump and interclump gas, for several illustrative species. In Table 1 we give the computed fractional abundances of potentially observable species in the clump, and also the clump:interclump ratio of abundances, for several epochs between about 2 and 10 thousand years, i.e. the period of transition from PPN to PN phases.

The figures show generally the same qualitative behaviour. A comparison of clump and interclump abundances shows that molecules are photodissociated earlier in the interclump than in the clump gas, as expected. Thus molecules survive longer in the clumps, and so the ratio of clump to interclump abundances varies strongly. For example, the CN abundance ratio varies from 0.26 at 2550 yr to 270 at 10050 yr, a factor of 1000.

Figure 1 shows the clump and interclump evolution of CO and CN fractional abundances. These represent molecules that have high and low initial abundances, respectively, i.e. in the stellar atmosphere of the AGB star. The abundance of CO remains high in both clump and interclump gas until photodissociation begins to play a role as the gas density and extinction decline during the expansion, with CO in the higher density clump gas surviving until later times. On the other hand, CN is a molecule formed as a product of photodissociation of larger species, here called a *degradation product*. Since photodissociation is faster in the interclump gas, the production of CN is also faster there initially, so CN rises faster in the interclump gas than in the clump, but also declines earlier.

Similar effects are observed for other species. The simple carbon chains C₄H and C₅H are both degradation products of larger species, and the time evolution illustrated in Figure 2 shows that their abundances peak in the interclump gas earlier (by several thousand years) than in the clump

Species	$X(\text{clump})$ $t = 2550 \text{ yr}$	$\frac{X(\text{clump})}{X(\text{interclump})}$ $t = 2550 \text{ yr}$	$X(\text{clump})$ $t = 6300 \text{ yr}$	$\frac{X(\text{clump})}{X(\text{interclump})}$ $t = 6300 \text{ yr}$	$X(\text{clump})$ $t = 10050 \text{ yr}$	$\frac{X(\text{clump})}{X(\text{interclump})}$ $t = 10050 \text{ yr}$
C	3.4×10^{-6}	1.4×10^{-2}	3.4×10^{-4}	2.4	6.0×10^{-4}	24
C ⁺	7.0×10^{-11}	6.0×10^{-6}	1.2×10^{-5}	1.1×10^{-2}	2.7×10^{-4}	0.22
CH	2.0×10^{-8}	8.9×10^{-2}	2.6×10^{-9}	0.65	4.4×10^{-9}	7.0
CH ⁺	1.8×10^{-15}	1.5×10^{-4}	5.8×10^{-14}	5.1×10^{-3}	1.8×10^{-12}	0.14
CO	9.1×10^{-4}	1.2	6.9×10^{-4}	18	1.8×10^{-4}	580
CN	5.1×10^{-6}	0.26	1.1×10^{-7}	55	9.4×10^{-10}	270
CS	1.1×10^{-5}	3.8	2.0×10^{-6}	1300	1.5×10^{-8}	3.3×10^4
SiC	7.0×10^{-7}	0.24	1.4×10^{-8}	260	4.6×10^{-11}	2.4
HCN	4.0×10^{-5}	22	1.0×10^{-10}	190	1.3×10^{-12}	21
HNC	1.4×10^{-8}	22	2.7×10^{-12}	5.3	2.2×10^{-12}	70
HCSi	5.3×10^{-8}	6.3×10^{-2}	1.8×10^{-8}	2200	6.2×10^{-11}	190
HCO ⁺	1.1×10^{-10}	0.27	4.4×10^{-12}	0.88	6.1×10^{-12}	7.1
SiCH ₂	1.6×10^{-8}	7.9	3.0×10^{-12}	6.5×10^5	1.2×10^{-16}	500
C ₂	1.0×10^{-6}	2.5×10^{-2}	2.6×10^{-7}	1.7	1.0×10^{-8}	45
C ₂ H	9.7×10^{-6}	0.47	3.8×10^{-8}	18	6.7×10^{-10}	79
C ₂ H ₂	2.1×10^{-7}	7.0	3.2×10^{-10}	610	2.9×10^{-12}	86
SiC ₂	6.4×10^{-6}	0.30	1.2×10^{-7}	1200	6.9×10^{-11}	2.0
SiC ₂ H	2.8×10^{-8}	4.0	1.1×10^{-10}	5.4×10^5	1.6×10^{-15}	1600
SiC ₂ H ₂	2.4×10^{-8}	4.8	9.4×10^{-11}	7.6×10^6	1.4×10^{-16}	470
C ₃	1.2×10^{-7}	0.28	9.7×10^{-8}	430	5.9×10^{-10}	1400
C ₃ H	7.1×10^{-7}	3.0	1.0×10^{-9}	460	1.3×10^{-12}	62
HC ₃ N	3.7×10^{-6}	4000	1.4×10^{-12}	3.9×10^4	1.1×10^{-15}	1.7×10^5
SiC ₃	1.2×10^{-7}	0.85	1.4×10^{-8}	110	4.3×10^{-13}	7.0×10^{-3}
C ₄	1.7×10^{-9}	2.4×10^{-3}	1.3×10^{-7}	300	6.0×10^{-12}	3.4
C ₄ H	6.0×10^{-9}	9.0×10^{-3}	1.6×10^{-8}	450	8.9×10^{-12}	92
SiC ₄	1.0×10^{-7}	3.0	4.2×10^{-11}	5.1×10^{-3}	5.1×10^{-18}	1.2×10^{-9}
C ₄ H ₂	2.2×10^{-9}	4.7×10^{-3}	1.5×10^{-10}	270	1.2×10^{-12}	22
C ₄ H ₃	6.4×10^{-6}	0.52	3.1×10^{-9}	3900	4.1×10^{-12}	90
C ₄ H ₄	2.2×10^{-8}	6.1×10^{-2}	3.0×10^{-6}	0.61	1.5×10^{-5}	1.8
C ₄ H ₅	6.6×10^{-5}	7.0	6.3×10^{-5}	13	5.1×10^{-5}	33
C ₅	4.6×10^{-10}	2.6×10^{-3}	1.1×10^{-7}	160	6.7×10^{-12}	1.7
C ₅ H	1.5×10^{-8}	1.4×10^{-2}	7.5×10^{-9}	2400	5.9×10^{-13}	39
C ₅ N	4.0×10^{-11}	2.5×10^{-3}	1.4×10^{-8}	7900	5.7×10^{-14}	1600
HC ₅ N	9.4×10^{-10}	5.3×10^{-2}	3.8×10^{-13}	2.4×10^4	1.6×10^{-17}	3600
C ₆	4.1×10^{-10}	5.5×10^{-3}	2.4×10^{-8}	130	1.9×10^{-14}	0.13
C ₆ H	1.0×10^{-7}	1.1	2.7×10^{-8}	34	3.0×10^{-14}	4.9×10^{-3}
C ₆ H ₂	1.8×10^{-8}	40	7.0×10^{-17}	87	1.1×10^{-18}	0.22
Benzene	2.6×10^{-8}	90	2.6×10^{-8}	90	2.6×10^{-8}	90
Benzyne	1.9×10^{-8}	7.1	1.9×10^{-8}	7.1	1.9×10^{-8}	7.1
C ₇	1.7×10^{-10}	1.1×10^{-2}	6.0×10^{-9}	630	1.1×10^{-14}	0.49
C ₇ H	5.0×10^{-8}	1.6	7.7×10^{-12}	1.2×10^4	2.9×10^{-18}	6.5
HC ₇ N	2.8×10^{-8}	6.1	1.5×10^{-15}	2.4×10^6	3.4×10^{-23}	33
O	2.0×10^{-6}	1.2×10^{-2}	2.2×10^{-4}	0.25	7.3×10^{-4}	0.80
Si	2.7×10^{-5}	12	5.0×10^{-7}	5.3	2.3×10^{-7}	4.2
SiO	3.4×10^{-8}	0.14	1.9×10^{-6}	1.2×10^5	1.1×10^{-10}	46
S	1.4×10^{-6}	0.12	2.4×10^{-6}	26	1.6×10^{-7}	2.3
SiS	9.6×10^{-6}	2.9	1.3×10^{-14}	3.8×10^4	1.2×10^{-17}	200
S ⁺	2.5×10^{-10}	7.5×10^{-5}	1.7×10^{-5}	0.80	2.2×10^{-5}	0.99

Table 1. Comparison of fractional abundances of potentially observable species at different times. The density, temperature and extinction at these times can be readily calculated from the equations in Section 2

gas. Figure 3 shows the time evolution of C₂H₂ (which is abundant in the stellar atmosphere) and C₄H₂, a degradation product of larger species. Their behaviours are as for CO and CN. Both molecules ultimately decline as the gas enters the interstellar medium.

Molecules with rather slower photodissociation rates survive longer. In Figure 4, benzene has a timescale for survival longer than the ten thousand year period considered here. This raises the possibility that some large and relatively photo-resistant species may survive the transition into the interstellar medium and may establish a popula-

tion there (Williams 2003). Note however that our benzene chemistry may be incomplete; in the chemistry adopted here its formation and destruction are mainly dominated by the neutral-neutral reaction of two C₃H₃ molecules and its reverse.

Table 1 illustrates the effects of the different photodissociation timescales in the expanding gas, and gives snapshot values of the clump:interclump abundance ratio at 2550, 6300, and 10050 yr, for species that are potentially observable. The earliest epoch is approximately when the interclump abundances are at a maximum, while the values in

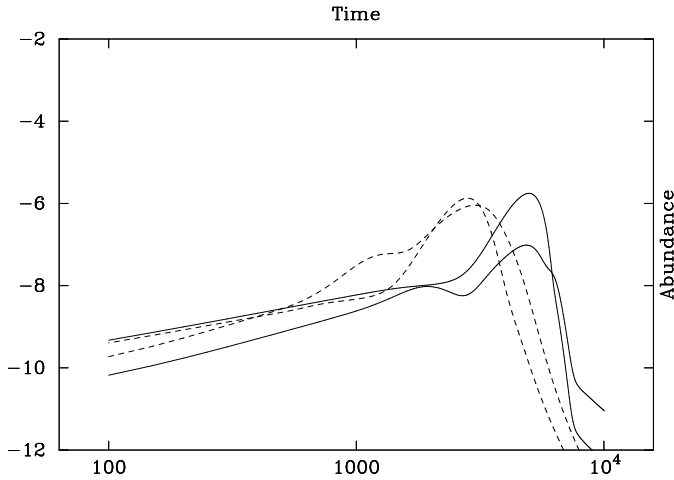


Figure 2. Clump (solid lines) and interclump (dashed lines) abundances for C_5H (uppermost solid line) and C_4H . The time is measured in years and the fractional abundance is with respect to the total number of hydrogen atoms.

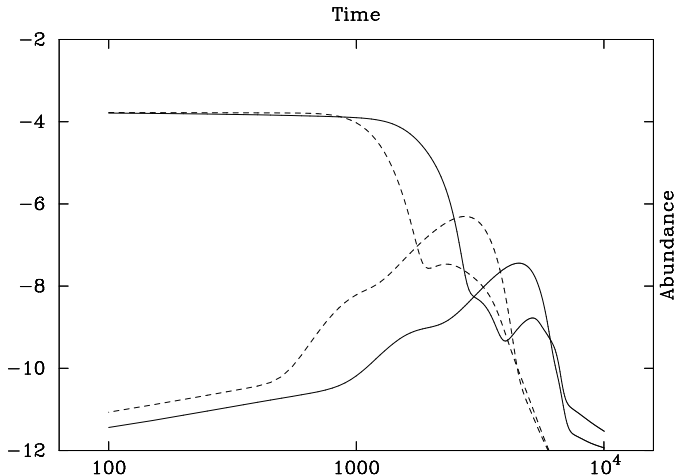


Figure 3. Clump (solid lines) and interclump (dashed lines) abundances for C_2H_2 (uppermost solid line) and C_4H_2 . The time is measured in years and the fractional abundance is with respect to the total number of hydrogen atoms.

the clump of species formed by degradation are low. For such species, then the ratio is low.

At epoch 6300 yr, many of the degradation products have declined in abundance in the interclump gas, while their abundances in the clump gas are growing, so the ratio is generally large. At the latest epoch shown in Table 1, then most of the degradation products have declined in abundance in the clump gas, and have declined even further in the interclump gas, so the ratio is in many cases again large. However, by this stage the abundances in the clump gas may have declined so far as to make many of the species undetectable. If we take a fractional abundance of 10^{-8} to represent a characteristic detection limit at 10000 yr, where the clump extinction is ~ 1 magnitude, then about 70% of the species listed are possibly not detectable at this epoch, whereas only about 30 percent are not detectable at 6500 yr. Thus, there is a very significant change in the detectable chemistry of the clump gas the PN ages.

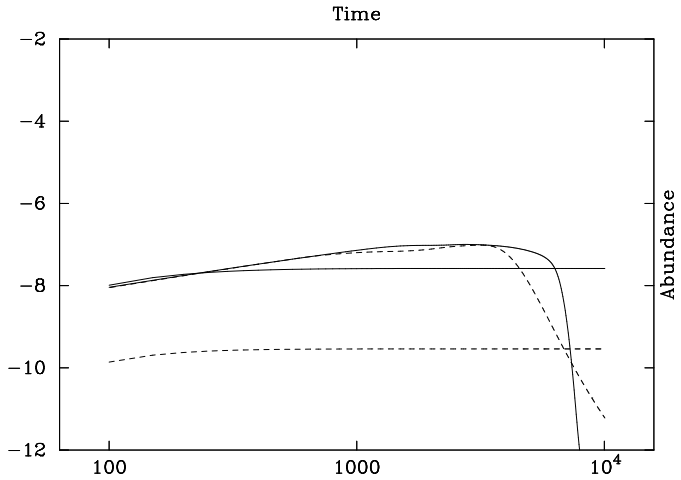


Figure 4. Clump (solid lines) and interclump (dashed lines) abundances for C_6H (uppermost solid line) and benzene. The time is measured in years and the fractional abundance is with respect to the total number of hydrogen atoms.

	Clump	Interclump
$X > 10^{-6}$ at 2550 yr	$CO, CS, HCN, C_3H, HC_3N, C_4H_5, SiS$	$CO, CN, SiC, C_2, C_2H, SiC_2, C_4H_3$
$X > 10^{-7}$ at 6300 yr	$CO, CS, HCN, C_3H, HC_3N, C_4H_5, SiS$	C_4H_4
$X > 10^{-8}$ at 10050 yr	CS, C_2, C_4H_4, C_4H_5	none

Table 2. List of important potential tracers of the clump and interclump gas at the three epochs

The column density of any species is made up of contributions from both clump and interclump gas. At the earliest PPN epoch illustrated, Table 1 shows that chemistry is largely determined by the interclump gas, while at later epochs it is determined in the clumps. Table 2 lists molecules that are likely to be the most important tracers of either clump or interclump gas, at the three epochs chosen.

3.2 Comparison with observations

Here the results will be compared very generally with observations of three objects: CRL618, NGC7027 and the Helix nebula. These objects span progressively advanced evolutionary stages with CRL618 being a PPN, NGC 7027 a young PN and the Helix an evolved PN. As discussed immediately below, comparison with CRL618 is made difficult by the complex geometry of the source. The comparisons with NGC 7027 and the Helix are more straight-forward.

Carbon-rich protoplanetary nebulae such as CRL618 and AFGL2688 have been the subject of several molecular studies in recent years. In particular, CRL618 has been used as a typical example of an asymptotic giant branch (AGB) star in the transition evolving toward the planetary nebula stage (Herpin & Cernicharo 2000; Cernicharo et al. 2001a,b; Woods et al. 2002). Here we attempt a qualitative comparison of our models with some observations and theoretical work on this object. Herpin & Cernicharo (2000) show that

to reproduce the observed emission of CO, HCN, HNC, H₂O, OH and O, a 3-component geometry is needed (see their figure 3), with a central torus at high density ($\sim 5 \times 10^7 \text{ cm}^{-3}$) and a gradient of temperatures ranging from 250 to 1000 K; an extended AGB remnant envelope with a density of $5 \times 10^5 \text{ cm}^{-3}$ and temperature of 100K; and finally the lobes, where high velocity gas is emitted from, with a density of 10^7 cm^{-3} and a two-component temperature of 200 and 1000 K. In follow up papers, Cernicharo et al. (2001a,b) observed methylpolyynes, small hydrocarbons and benzene along the same line of sight and conclude that the emission of these species must come from the central torus region.

The scenario we model is different from the 3-component geometry but we can attempt a comparison with the species emitted from the AGB remnant component where the temperature is close to the one derived in our model (see Table 1), although the density is much higher. We find that our best match with the PPN CRL618 occurs at early times \sim few hundred years. At this time the density is relatively high: our CO column density is $6 \times 10^{18} \text{ cm}^{-2}$, while Herpin & Cernicharo (2000) derive a value of $7 \times 10^{18} \text{ cm}^{-2}$ and our HCN is $2.5 \times 10^{17} \text{ cm}^{-2}$, only slightly over a factor of 4 less than the observed one; our HNC is, however, over 3 orders of magnitude underabundant with respect to observations. Given the differences in the physical parameters adopted, any further comparison would be of limited value.

It should also be noted that following the ISO discovery of benzene in CRL618 (Cernicharo et al. 2001b), Woods et al. (2002) presented a chemical model of this proto-planetary nebula. They show that the physical conditions of CRL618 are such to encourage an efficient production of benzene. However, similarly to Cernicharo et al. (2001b) results, they model the dense inner torus and therefore we are unable to make a direct comparison with their chemical model.

The young PN NGC 7027 is molecule rich with a large number of species identified within it. Hasegawa & Kwok (2001) have observed several species and collated the results of previous work. In their table 3, they list measured fractional abundances. If the emission that Hasegawa & Kwok (2001) detected is regarded as originating from a large collection of clumps then their results can be directly compared with ours in Table 1. Adopting an age of around 1000 yr for the nebula and comparing with our results gives the following: CN is predicted to have a fractional abundance of 9×10^{-10} and Hasegawa & Kwok (2001) measure 1.7×10^{-8} ; HCN is 6×10^{-5} (predicted) verses $> 1.2 \times 10^{-9}$ (observed); and C₂H is 6×10^{-7} vs 1.1×10^{-8} . Given the simplicity of the model and the inexactness of the comparison to be within around one order of magnitude of the observational results for several species is very encouraging (the exact age of the nebula or the filling factor of the clumps can easily yield uncertainties of an order of magnitude).

To compare the results for the later stages with those of the Helix, we can use the last columns of Table 1 with the results of Bachiller et al. (1997). The model results for this evolved PN do not agree nearly so well with the observations as for NGC7027 and CRL618. Some results are not inconsistent with the observations: the model predictions do not exceed the upper limits established for SiO and CS, being an order of magnitude less; the predicted HC₃N abundance is several orders of magnitude less than the upper limit set by

Bachiller et al. (1997). However the models severely underpredict the abundances of HCN, HNC, CN and HCO⁺. This indicates that these molecules whose earlier clump abundances were comparable to the observed levels survive for longer than our simple model predicts.

4 CONCLUSIONS

The chemistry of the gas in the slow wind ejected from a star in the AGB phase is strongly affected by photoprocesses driven by the hardening radiation field of the central star, as the system is transformed into a PPN and then to a PN. If the slow wind density distribution is smoothly monotonic, then the degradation product molecules in the gas are confined to the PPN stage. However, if the slow wind is clumpy, perhaps because of clumpiness in the precursor AGB atmosphere, then molecules in clumps are protected against photodissociation until significantly later times, and may be present in the PN phase of evolution. We have presented lists of molecules that may represent tracers of such clumpiness. Benzene survives the transition into the PN phase, suggesting that some long-lived molecules may last long enough to be injected into the general interstellar medium. A comparison with observations suggests that this model can, at the PPN and young PN stage, correctly predict the abundance of several molecular species to within an order of magnitude. At later stages, the model severely underestimates the abundance of some short-chain molecules. Thus the shielding of molecules in clumps may be even more effective than as described in this simple model.

The original aim of this work was to chemically identify when clumps form in PNe. The comparison of the results in the early stages with the data from CRL618 and NGC 7027 supports the hypothesis that the clumps form at an early stage; if they formed later out of low extinction gas, the abundances of the molecules would be significantly depleted compared with the values observed. As noted above, the evidence of the continuing presence of molecules in an evolved PN like the Helix indicates that the protective ability of the clumps persists until late stages. Future work in this field should include a more realistic physical model for the different post-AGB phases to account for the survival of molecules in the clumps. It should also be possible to model individual sources and thus carry out a much more detailed comparison with observations both from existing facilities and also from forthcoming facilities such as ALMA.

ACKNOWLEDGEMENTS

We thank the referee, Pierre Cox, for a very constructive report that led to an improved paper. We also thank John Dyson and Jonathan Rawlings for useful discussions. MPR acknowledges the support of PPARC. SV thanks the Italian Space Agency (ASI) and DAW thanks the Leverhulme Trust for financial support. PC was a Fellow supported by the European Commission TMR programme in Astrophysical Chemistry while this work was carried out.

REFERENCES

Bachiller R., Forveille T., Huggins P. J., Cox P., 1997, *A&A*, 324, 1123

Capriotti E. R., 1973, *ApJ*, 179, 495

Cau P., 2001, PhD thesis, UMIST, Manchester, UK

Dyson J. E., Hartquist T. W., Pettini M., Smith L. J., 1989, *MNRAS*, 241, 625

Frenklach M., Feigelson E. D., 1989, *ApJ*, 341

Garcia-Segura G., Franco J., 1996, *ApJ*, 469, 171

Hasegawa T. I., Kwok S., 2001, *ApJ*, 562, 824

Herpin F., Cernicharo J., 2000, *ApJ*, 530, L129

Howe D. A., Hartquist T. W., Williams D. A., 1994, *MNRAS*, 271, 811

Howe D. A., Millar T. J., Williams D. A., 1992, *MNRAS*, 255, 217

Huggins P. J., Mauron N., 2002, *A&A*, 393, 273

Martin-Pintado J., Gaume R. A., Johnston K. J., Bachiller R., 1995, *ApJ*, 446, 687

Mauron N., Huggins P. J., 2000, *A&A*, 359, 707

Meaburn J., Clayton C. A., Bryce M., Walsh J. R., Holloway A. J., Steffen W., 1998, *MNRAS*, 294, 201

Millar T. J., Farquhar P. R. A., Willacy K., 1997, *A&AS*, 121

O'Dell C. R., Balick B., Hajian A. R., Henney W. J., Burkert A., 2002, *AJ*, 123, 3329

O'Dell C. R., Handron K. D., 1996, *AJ*, 111, 1630

Shu F., 1991, *Physics of Astrophysics*, Vol. II: Gas Dynamics. University Science Books, New York.

Viti S., Williams D. A., 1999, *MNRAS*, 310, 517

Williams R. J. R., 1999, *MNRAS*, 310, 789

Young K., Cox P., Huggins P. J., Forveille T., Bachiller R., 1997, *ApJ*, 482, L101